Are sucrose transporter expression profiles linked with patterns of biomass partitioning in *Sorghum* phenotypes?

Ricky J. Milne[1], Caitlin S. Byrt[1,2], John W. Patrick[1] and Christopher P. L. Grof[1]*

[1] School of Environmental and Life Sciences, University of Newcastle, Newcastle, NSW, Australia
[2] Australian Research Council Centre of Excellence in Plant Cell Walls, Waite Campus, University of Adelaide, Adelaide, SA, Australia

Sorghum bicolor is a genetically diverse C_4 monocotyledonous species, encompassing varieties capable of producing high grain yields as well as sweet types which accumulate soluble sugars (predominantly sucrose) within their stems to high concentrations. Sucrose produced in leaves (sources) enters the phloem and is transported to regions of growth and storage (sinks). It is likely that sucrose transporter (SUT) proteins play pivotal roles in phloem loading and the delivery of sucrose to growth and storage sinks in all *Sorghum* ecotypes. Six *SUTs* are present in the published *Sorghum* genome, based on the BTx623 grain cultivar. Homologues of these *SUTs* were cloned and sequenced from the sweet cultivar Rio, and compared with the publically available genome information. SbSUT5 possessed nine amino acid sequence differences between the two varieties. Two of the remaining five SUTs exhibited single variations in their amino acid sequences (SbSUT1 and SbSUT2) whilst the rest shared identical sequences. Complementation of a mutant *Saccharomyces* yeast strain (SEY6210), unable to grow upon sucrose as the sole carbon source, demonstrated that the *Sorghum* SUTs were capable of transporting sucrose. *SbSUT1*, *SbSUT4*, and *SbSUT6* were highly expressed in mature leaf tissues and hence may contribute to phloem loading. In contrast, *SbSUT2* and *SbSUT5* were expressed most strongly in sinks consistent with a possible role of facilitating sucrose import into stem storage pools and developing inflorescences.

Keywords: expression profiling, *Sorghum*, source–sink pathway, sucrose transporters, sucrose storage

INTRODUCTION

The storage of organic carbon as non-structural carbohydrates by plants is of biological and commercial interest. In this context, many varieties exist within the genetically diverse *Sorghum bicolor* species ranging from grain *Sorghum* types which store large amounts of starch within their grains to sweet *Sorghum* types which accumulate sucrose/hexoses within their stems. Sweet *Sorghum* cultivars are capable of accumulating soluble sugars up to 60% of their internode dry weight (Hoffmann-Thoma et al., 1996). The Rio cultivar can accumulate three times the amount of sugar (total glucose, fructose, and sucrose g/kg stem tissue) in mature stems compared to grain *Sorghum* cv. BTx623 (Murray et al., 2008). For these reasons, sweet *Sorghum*, a C_4 monocotyledonous plant with high yield potential, is regarded as an ideal feedstock to provide sugar for bioethanol production. Higher sugar lines are preferred for the production of "first generation" bioethanol. A high sugar variety may yield 500 g of sugar per kg of stem dry weight, and total soluble sugar yields can reach 10 t ha^{-1} (Zhao et al., 2009). These yields equate to theoretical ethanol yields of up to 5414 L ha^{-1} (Zhao et al., 2009). However, higher sugar, and hence ethanol yields per hectare may be achievable through selective breeding and/or genetic transformation of *Sorghum*.

During sugar accumulation within stems, sucrose produced in photosynthetic source leaves is transported within phloem sieve element-companion cell (SE-CC) complexes to an array of sinks (non-photosynthetic organs) comprising developing vegetative and reproductive organs (growth sinks) as well as the stem storage sink. Within growth sinks carbohydrates are invested primarily into the biosynthesis of cellular structures. In contrast, elongating and mature internodes of cv. Rio accumulate sucrose within vacuoles, cytosols, and apoplasmic spaces of their storage parenchyma cells (Lingle, 1987).

In the C_4 species maize (*Zea mays*), closely related to *Sorghum*, sucrose loading of SE-CC complexes occurs apoplasmically (Slewinski et al., 2009). It is assumed that a similar pathway of phloem loading of sucrose is followed in *Sorghum*. In stems of sugarcane and *Sorghum*, sucrose is transferred radially from their SE-CC complexes into storage parenchyma cells. Intracellular compartmentation of stored sucrose in *Sorghum* is presumed to be similar to that of sugarcane. Here, the bulk of sucrose accumulates within vacuoles of their storage parenchyma cells to concentrations that equal or exceed sucrose concentrations of the phloem sap. Thus the possibility of a concentrating step is invoked. Since the pathway of phloem unloading follows a symplasmic pathway in sugarcane stems (Jacobsen et al., 1992), any concentrating step must be localized to tonoplasts of their storage parenchyma vacuoles. Inconsistent with this conclusion is the finding that sucrose transport into isolated vacuoles of sugarcane stems occurs by facilitated diffusion (Williams et al., 1990; Preisser and Komor, 1991). However, whether an energy-dependent transport step operates in parallel with facilitated diffusion into vacuoles, as reported

for sugar beet (Saftner et al., 1983), remains to be resolved for sugarcane. In the case of *Sorghum*, the phloem unloading pathway of sucrose into stem storage parenchyma cells appears to include an apoplasmic component (Tarpley and Vietor, 2007) and hence an additional reliance on movement across plasma membranes arranged in series with tonoplast transport.

Import of sucrose into cells across their plasma membranes is mediated by sucrose transporters (SUTs). SUTs are energy-dependent trans-membrane proteins which co-transport sucrose and protons in the same direction, in a 1:1 stoichiometric ratio (Lalonde et al., 2004). Therefore, *Sorghum* SUTs are of interest because they may play key roles in apoplasmic phloem loading of sucrose in source leaves and apoplasmic unloading of sucrose into stem storage sinks (see above). SUTs are known to function in phloem loading of maize source leaves (Slewinski et al., 2009) but the role of SUTs in stem storage is less certain. Here the final sucrose concentration within stems can be a balance between import and remobilization to provide a supplementary source of organic carbon to support grain filling when leaf photosynthesis has been depressed by stressful conditions (Blum et al., 1994, 1997). However, remobilization of stem reserves in a number of *Sorghum* cultivars has been reported to be minimal under favorable environmental conditions (Gutjahr et al., 2013).

Here we investigate the expression of *Sorghum* SUTs in source and sink organs during vegetative growth and at anthesis in two cultivars of *Sorghum*, cv. BTx623 and cv. Rio. These two cultivars exhibit very different phenotypes, with cv. BTx623 being of short stature and producing a large grain head. In contrast, cv. Rio produces a small panicle with fewer grains, but may grow to a height of 3 m with a stout culm for sugar storage. Differences in *SUT* expression between cultivars may correlate with phloem loading, long distance transport, and ultimately partitioning of sucrose to reproductive sinks in cv. BTx623 or stem sinks in cv. Rio. Complementation of the deficient *Saccharomyces cerevisiae* SEY6210 strain by *Sorghum* SUTs is also explored as a first step toward detailed functional characterization of these transporters.

MATERIALS AND METHODS

PLANT GROWTH CONDITIONS
Seeds of the *Sorghum* cultivars Rio and BTx623 were germinated and grown in 10 L pots containing a soil mixture consisting of two parts coarse sand, one part coco peat, and one part perlite, under glass house conditions with temperatures maintained at $25.5 \pm 1.5°C$ during the day, and $15.5 \pm 0.5°C$ during the night. Plants were exposed to a photoperiod of 14-h light and 10-h dark cycle with supplementary lighting provided by tungsten incandescent lamps. Seedlings were thinned to one per pot at 1-week post germination. Pot water levels were maintained at field capacity with a programmable drip irrigation system delivering water to each pot for two min, three times per day. Osmocote exact slow release fertilizer (Scotts Australia Pty Ltd, Sydney, NSW, Australia) was applied at a rate of 20 g per pot 2-weeks post germination and was supplemented with liquid fertilizer (Wuxal Liquid Foliar Nutrients; AgNova Technologies Pty Ltd, Eltham, VIC, Australia) at fortnightly intervals. Nitrogen (N), phosphorus (P), and potassium (K) ratios for Osmocote exact were 15N, 3.9P, and 9.1K.

HARVESTING PLANT MATERIAL
All plant samples were snap frozen in liquid nitrogen immediately following harvest. During the vegetative growth phase, cv. BTx623 (grain) and cv. Rio (sweet) were destructively harvested approximately 60 and 90 days after germination, respectively. Material harvested for analysis was a sink leaf (expanding leaf fully enclosed within leaf sheaths); source leaf (youngest fully expanded leaf), internode 2 (elongated internode; numbered acropetally), and internode 5 (elongating). At anthesis, cv. BTx623 and cv. Rio were harvested approximately 103 and 140 days after germination, respectively. The flag leaf and leaf 7 (numbered acropetally), the flag internode, internode 2 and whole inflorescences were harvested. Additional samples were taken for detailed analysis of SUT expression. These were upper portion (5 cm) of the flag internodes and inflorescences separated into spikelets, anthers, and rachis branches.

ISOLATION OF TOTAL RNA
Tissue samples were cryogenically ground in stainless steel grinding jars cooled on dry ice with a cooled stainless steel ball bearing agitated for 1 min at 30 Hz using a Retsch TissueLyser II (QIAGEN, Chadstone Centre, VIC, Australia). Total RNA was isolated from 100 mg of ground material. Leaves were extracted using the plant RNeasy® kit (QIAGEN) whilst stems and inflorescences were extracted using the plant RNA reagent (Life Technologies, Mulgrave, VIC, Australia). Digestion of contaminating genomic DNA was performed post RNA isolation using the Ambion® TURBO™ DNase kit (Life Technologies). RNA isolation and genomic DNA digestions were performed according to the manufacturer's instructions.

SYNTHESIS OF cDNA
Complementary DNA (cDNA) was synthesized from 1 µg of RNA using the Thermoscript® first strand cDNA synthesis kit (Life technologies) with an oligo d(T) primer, at an extension temperature of 60°C, according to the manufacturer's instructions.

CLONING FULL-LENGTH GENES
Full-length coding DNA fragments of each *Sorghum SUT* was cloned from cDNA by polymerase chain reaction (PCR) using Fermentas 2xMM (ThermoFisher, Scoresby, VIC, Australia) spiked with 1 µL Fermentas Pfu polymerase (ThermoFisher) using gene specific primers (**Table 1**). PCR cycling conditions were 95°C for 10 min followed by 35 cycles of 95°C for 30 s, 55°C for 30 s, 72°C for 2 min (2 min 20 s for *SbSUT2*). Amplified products were cloned into the pGEM-t easy vector (Promega, Sydney, NSW, Australia) and at least three clones were sequenced from separate cDNA samples. *SUTs* were then amplified from plasmids using the Stratagene Pfu Ultra II polymerase (Integrated Sciences, Chatswood, NSW, Australia) by primers incorporating restriction sites at the start and stop codons as shown in **Table 1** and recommended cycling profile using a 55°C annealing temperature. Products were digested with corresponding FastDigest® Fermentas restriction enzymes (ThermoFisher), as were the yeast expression vectors. *SUTs* were then ligated into pDR195 (*SbSUT5* and *SbSUT6*) or pDR196 (Rentsch et al., 1995).

Table 1 | Primer sets used for PCR amplification of *Sorghum SUT*s. Restriction site sequences are underlined.

Gene	Forward primer (5′–3′)	Reverse primer (5′–3′)
Full-length primers		
SbSUT1	GTCGTCCCGTACGTGTGC	ATCTTGCACGGTTGGGTTT
SbSUT2	CCGCAGCGACACCTACAC	AATGGCAAAATGGGGCTAAGT
SbSUT3	CTCCACACCTCTCCGGTTT	CGACAGTAGTGGTTGATCG
SbSUT4	TCAAAGCAACTCAGCGATTC	AGCTGCAACTCTTCCAAAGC
SbSUT5	GTAGCCATGGACGGTGGTG	CCGCCTGGCGATAGATAGAT
SbSUT6	CGTTCCTGCTCCTCTCACTC	TGGATTTCCGATCATCCACT
Restriction cloning primers		
SbSUT1	CTCGCGGAATTCATGGCTCGCGGCGA EcoRI	GGCCGTGTCGACTCAGTGGCCGCCCG SalI
SbSUT2	GGCGCGGTCGACATGGACGCCGGCACC SalI	TTGGGCAGTCGACTCAGCCAAATCCATGG XhoI
SbSUT3	CCGGTTGAATTCATGGCTGCTGATGGC EcoRI	CTGGACCTCGAGTCAATGGCCTCCTC XhoI
SbSUT4	CCGTGAGAATTCATGCCGCCGCGCAC EcoRI	GTAATGAGTCGACTTATCGGTGCGTGC SalI
SbSUT5	AATTCGAGCGGCCGCATGGACGGTGGTGAC NotI	GCGATAGGATCCTCAGTGGCCGCCGC BamHI
SbSUT6	GCCCGGCGGCCGCATGGACGACGGTGAC NotI	CCTGGAGGATCCTCAACAGTGGCCGC BamHI
qPCR primers		
SbSUT1	GTGCTCCTGTAATCTTTGTGTCC	ACTATACTGCACATTGATTGATCG
SbSUT2	GCACATGCATTGAATGAACC	TTCGCATTTGGAAATTCCTC
SbSUT3	GGCCGGATCAAACAAGAT	GGCATTGCGAAGGAATGA
SbSUT4	CGATCCATGATGATGTCCAG	GTTCCAGGCCTTGCTGTC
SbSUT5	CCCGTAGTGTTGCGGAGTC	CCAATGGATCGGAAAATAAAG
SbSUT6	GCACAACAGCACAAAGAAGG	AGGCAGAAGAGGCTGAGATG
SbGAPDH	AGGGTATCATGGGCTACGTG	AGTTGTCGTTCAGGGCAATC
SbEF1a	CATGGTGGTGGAGACCTTCT	TCCTTCTTCTCCACGCTCTT

YEAST TRANSFORMATION

Sorghum SUT-yeast expression vector constructs were introduced into the *Saccharomyces cerevisiae* yeast strain SEY6210 (MATα leu2–3, 112 ura3–52 his3−Δ200 trpl-Δ901 lys2–801 suc2- Δ9 GAL; Robinson et al., 1988) using the 40% PEG1000 transformation method (Dohmen et al., 1991). Yeast transformants harboring one of each of the cv. Rio SUTs, the cv. BTx623 SbSUT5 (SbSUT5G) and empty pDR196 vector were identified. Media lacking uracil was used for selection as the pDR yeast expression vectors contain the uracil synthesis gene. DNA was extracted from yeast post transformation, then plasmids were transformed into *Escherichia coli* (strain DH5α), and were harvested using a Plasmid Mini Kit (QIAGEN). Plasmids were sequenced to confirm that the *SUT* sequences were correct. In short, 1.5 mL yeast culture was pelleted, washed with MilliQ water then resuspended in lysis buffer [50 mM Tris-HCl pH 8, 100 mM NaCl, 1% SDS, 2% Triton X-100,

1 mM ethylenediaminetetraacetic acid (EDTA)]. Glass beads were added (0.3 g, 425–600 μm diameter) along with 200 μL phenol:chloroform:isoamyl alcohol (25:24:1; Sigma-Aldrich, Castle Hill, NSW, Australia) and vortexed for 10 min followed by microcentrifugation for 5 min at maximum speed. The upper extract layer was then removed and DNA precipitated in 1 mL ethanol prior to pelleting and resuspension in 50 μL TE.

YEAST COMPLEMENTATION

Transformed yeast strains harboring *Sorghum* SUTs, empty pDR196 and PsSUT1 were grown in liquid culture to an OD_{600} of 0.8 in synthetic dropout media lacking uracil. Untransformed yeast was cultured in synthetic complete media. Yeast were streaked (2 μL) on solid media lacking uracil and supplemented with either sucrose (25 mM) or glucose (100 mM) as the sole carbon source. This was repeated three times and plates were photographed

using a ChemiDoc™ XRS system (Bio-Rad, Gladesville, NSW, Australia). SuSy7 yeast harbouring PsSUT1-pDR196 was kindly provided by Zhou et al. (2007) for use as a positive control.

SUT TRANSCRIPT QUANTIFICATION BY qPCR

Primers used for quantitative PCR (qPCR; **Table 1**) were designed to amplify regions of the 3′ UTR of each *SUT* due to high sequence homology within coding regions, with the exception of *SbSUT2* where a region from the coding sequence was amplified. Products from standard PCR were sequenced to ensure that correct gene fragments were amplified. Quantitative PCR was carried out on a Rotor-Gene Q (QIAGEN) using the QuantiFast SYBR green PCR kit (QIAGEN) and a two-step cycling program according to the manufacturer's instructions. The green channel was used for data acquisition. Gene expression was measured relative to the housekeeper, *Sorghum bicolor elongation factor 1-alpha* (*SbEF-1α*).
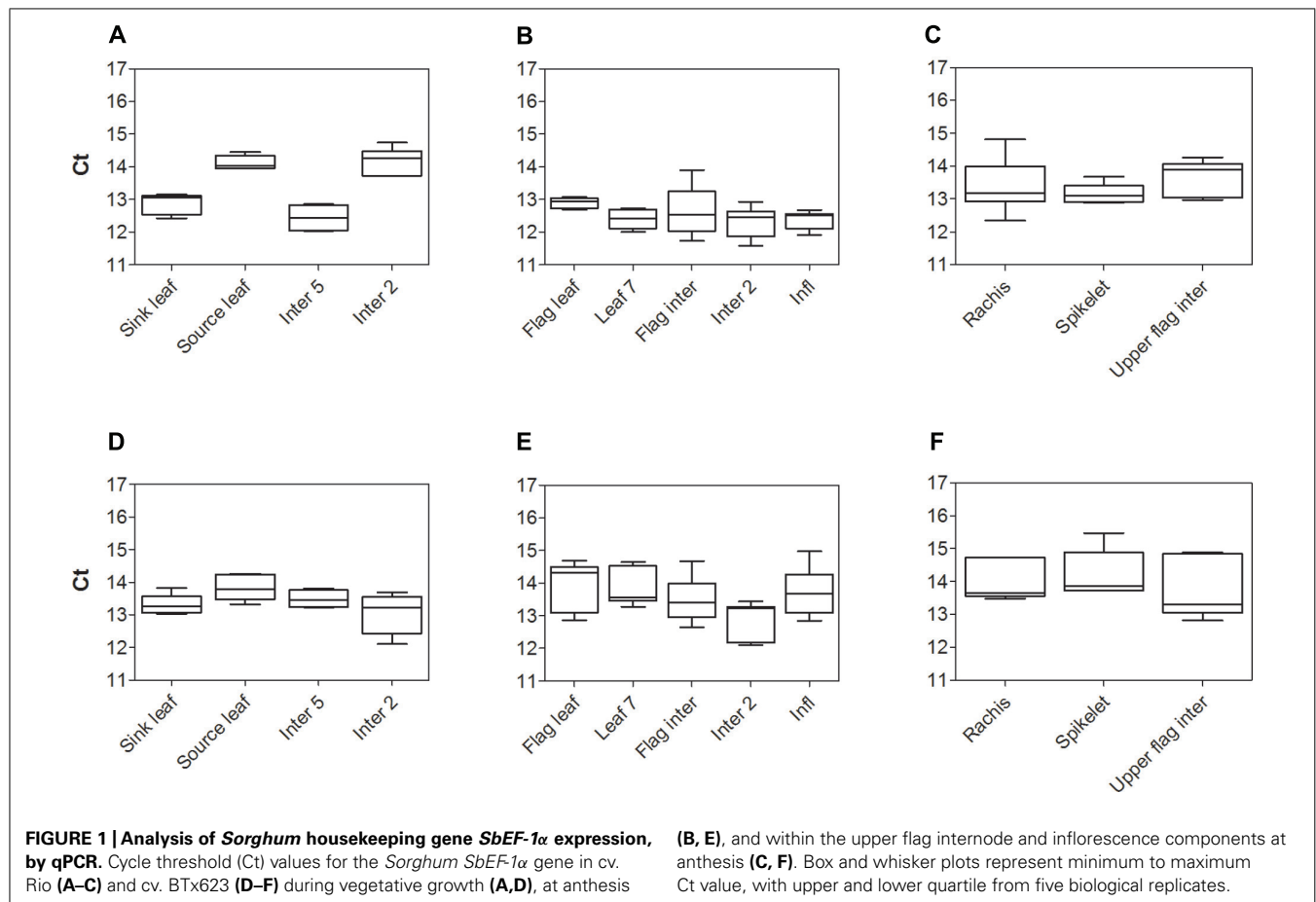
SELECTION OF HOUSEKEEPING GENE FOR qPCR

The expression stability of two widely used housekeeping genes, *Sorghum bicolor glyceraldehyde-6-phosphate dehydrogenase* (*SbGAPDH*) and *SbEF-1α* from cv. Rio, were assessed prior to measuring expression levels of *Sorghum SUTs*. Comparison of cycle threshold values (Ct) and ab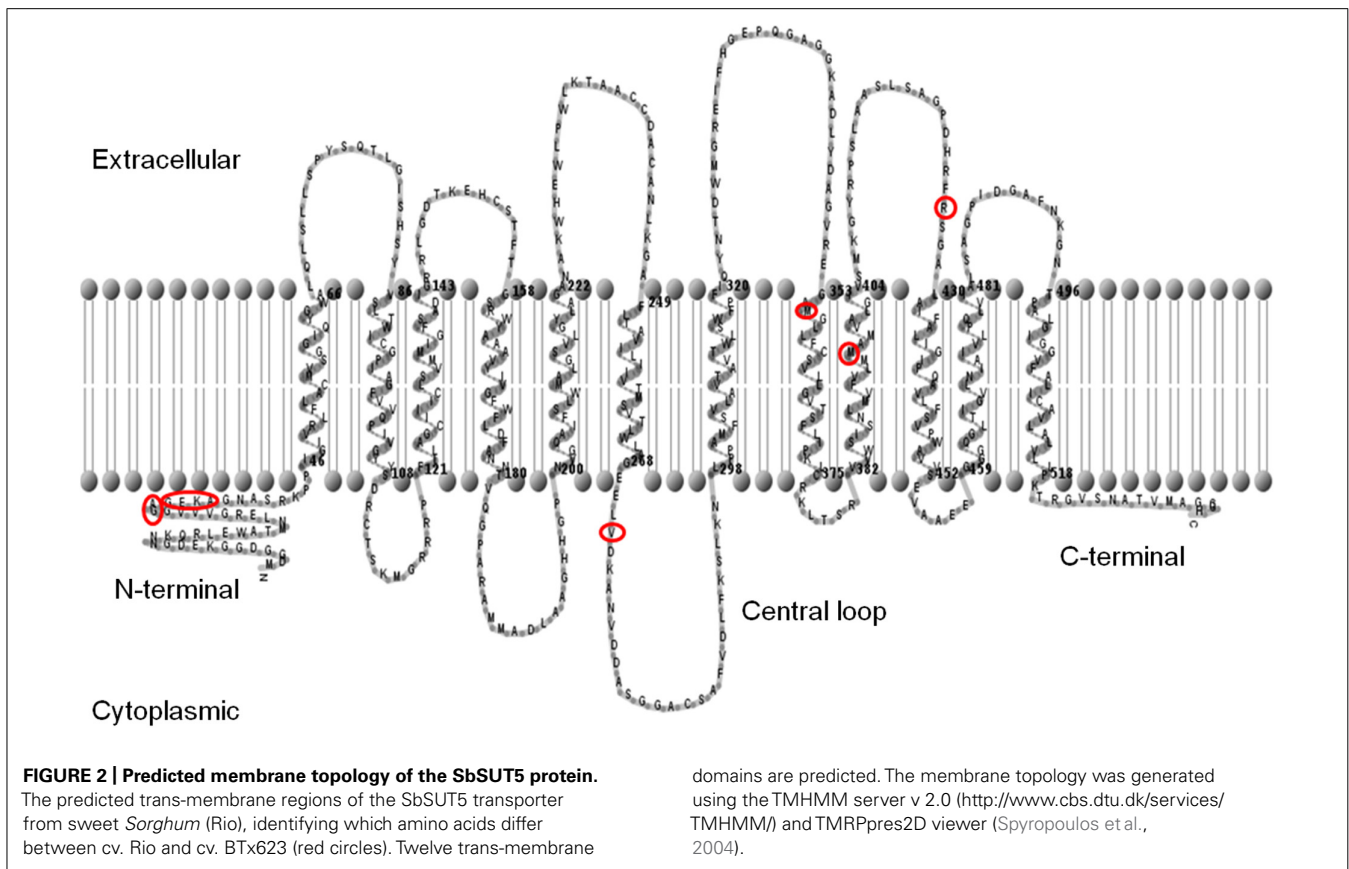solute expression levels (data not shown) revealed both housekeeping genes were quite stably expressed within each organ examined. However, differences in expression of *SbGAPDH* were greater than those for *SbEF-1α*. Hence *SbEF-1α* was chosen to normalize *SUT* expression in subsequent experiments. The stability of *SbEF-1α* was compared between cv. BTx623 and cv. Rio (**Figure 1**). Expression of *SbEF-1α* was least stable in cv. Rio during vegetative growth (Source leaf and Inter 2 – **Figure 1A**) and cv. BTx623 at anthesis (Inter 2 – **Figure 1E**). However, in all cases this variation was insignificant relative to the observed genotypic differences in the relative expression levels of the genes of interest and hence had no impact on the conclusions drawn.

RESULTS

SbSUT SEQUENCES

Full-length coding sequences of each *SUT* from both *Sorghum* cultivars were amplified by PCR, cloned, and then sequenced. Twelve trans-membrane domains were predicted for each SUT using the TMHMM (Hidden Markov model-based transmembrane) predictive algorithm, and a graphical representation of the membrane topology of SbSUT5 is shown (**Figure 2**). Cytoplasmic N- and C-termini were predicted along with a central loop domain. Sequence analysis (not shown) revealed that a number of conserved features are present in *Sorghum* SUTs. A conserved histidine residue is present in the first loop domain corresponding to

FIGURE 1 | Analysis of *Sorghum* housekeeping gene *SbEF-1α* expression, by qPCR. Cycle threshold (Ct) values for the *Sorghum SbEF-1α* gene in cv. Rio **(A–C)** and cv. BTx623 **(D–F)** during vegetative growth **(A,D)**, at anthesis **(B, E)**, and within the upper flag internode and inflorescence components at anthesis **(C, F)**. Box and whisker plots represent minimum to maximum Ct value, with upper and lower quartile from five biological replicates.

FIGURE 2 | Predicted membrane topology of the SbSUT5 protein.
The predicted trans-membrane regions of the SbSUT5 transporter
from sweet *Sorghum* (Rio), identifying which amino acids differ
between cv. Rio and cv. BTx623 (red circles). Twelve trans-membrane
domains are predicted. The membrane topology was generated
using the TMHMM server v 2.0 (http://www.cbs.dtu.dk/services/
TMHMM/) and TMRPpres2D viewer (Spyropoulos et al.,
2004).

His-65 (Lu and Bush, 1998) and amino acids which correspond
to the G-X-X-X-D/E-R/K-X-G-[X]-R/K-R/K motif reside in the
second and eighth loop domains (Lemoine, 2000; Pazdernik et al.,
2000). Only SbSUT4 contained an LXXLL motif in the N-terminal
domain, indicating it may be targeted to the tonoplast (Yamada
et al., 2010).

A number of amino acid differences were noted between cv. Rio
SUTs and the published cv. BTx623 genomic sequence. To examine
this further, *SUTs* from cv. BTx623 were cloned and sequences ver-
ified. SbSUT1 and SbSUT2 possessed single amino acid sequence
differences, whereas SbSUT3, SbSUT4, and SbSUT6 were identical
when sequences from cv. Rio and cv. BTx623 were aligned. SbSUT1
from cv. Rio had a valine (V) at position 381, whereas cv. BTx623
had an isoleucine (I) in this position. In SbSUT2 at amino acid 41, a
threonine (T) was present in the sequence from cv. Rio, but absent
in the cv. BTx623 sequence. SbSUT5 exhibited the most variation
between the two cultivars with nine amino acid differences. Five
amino acids out of a string of six differed between cv. BTx623 and
cv. Rio SUT5, and were predicted to lie in the N-terminal region
of the transporter (**Figure 2**). Starting at amino acid 32, the cv.
Rio sequence predicted GAGEKA whilst the cv. BTx623 sequence
predicted AGEKKG. Single amino acid differences between the
cv. Rio and cv. BTx623 sequences occurred at amino acid 272,
355, 396, and 426 as shown in **Figure 2** (V272L; M355V; M396T,
and R426K, respectively). These amino acid sequence differ-
ences in the SUTs between the two cultivars are summarized in
Table 2.

**Table 2 | Summary of SUT sequence variation between BTx623 and
Rio cultivars.**

SUT	No. of variations (BTx623 vs Rio)	Amino acid variations
SbSUT1	1	I381V
SbSUT2	1	T41 insertion (Rio)
SbSUT3	0	–
SbSUT4	0	–
SbSUT5	9	A32G, G33A, E34G, K35E, G37A, L272V, V355M, T396M, K426R
SbSUT6	0	–

PHYLOGENETIC ANALYSIS OF MONOCOTYLEDONOUS SUTs
A phylogenetic analysis demonstrated that the *Sorghum* SUTs clus-
tered into four clear groups (**Figure 3**). This is consistent with
phylogenetic analyses of other grass species including the C_3,
Lolium perenne (Berthier et al., 2009) and the C_4 *Zea mays* (Braun
and Slewinski, 2009). Two transporters appeared in Groups 1
and 5. In previous studies, Group 2 contained only SUTs from
eudicots (Berthier et al., 2009; Braun and Slewinski, 2009). The
Sorghum SUTs aligned closely with SUTs from other C_4 mono-
cotyledonous species such as maize, sugarcane, and *Setaria viridis*
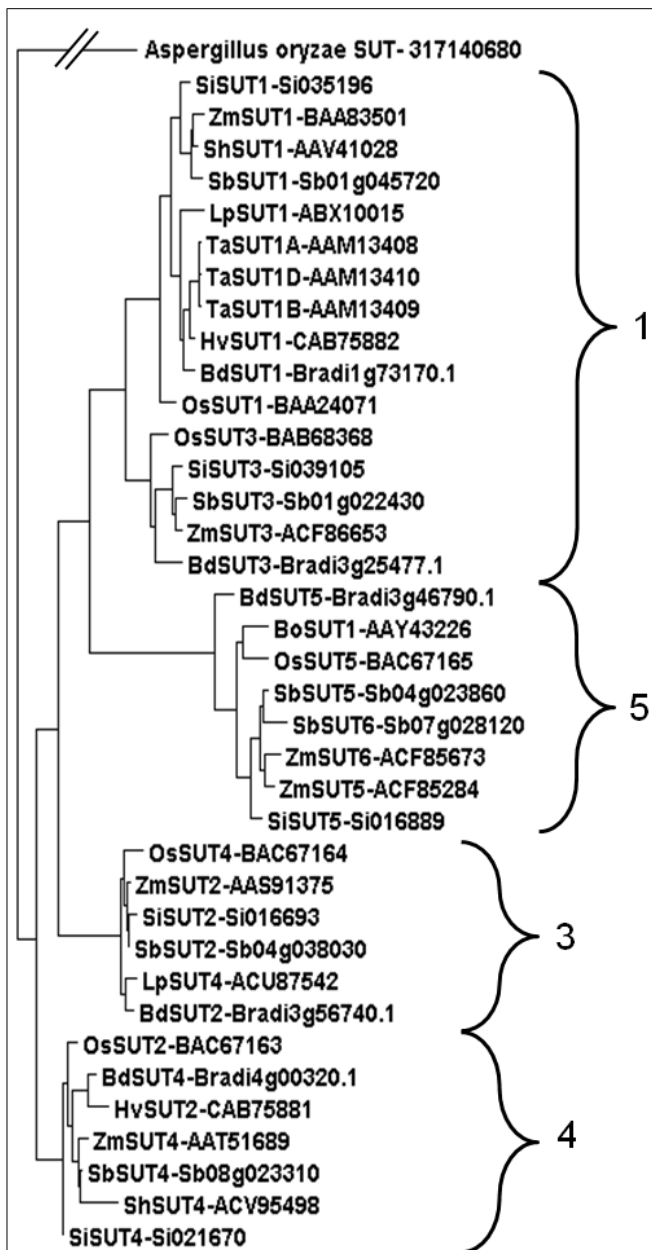(**Figure 3**).

FIGURE 3 | Phylogenetic analysis of SUTs from monocotyledonous species. SUTs displayed fit into Groups 1, 3, 4, 5 (Braun and Slewinski, 2009) from species *Brachypodium distachyon*** (BdSUT1, BdSUT2, BdSUT3, BdSUT4, BdSUT5), *Bambusa oldhamii* (BoSUT1), *Hordeum vulgare* (HvSUT1, HvSUT2), *Lolium perenne* (LpSUT1, LpSUT4), *Oryza sativa*** (OsSUT1, OsSUT2, OsSUT3, OsSUT4, OsSUT5), *Saccharum* hybrid (ShSUT1, ShSUT4), *Setaria italica*** (SiSUT1, SiSUT2, SiSUT3, SiSUT4, SiSUT5), *Sorghum bicolor*** (SbSUT1 – Sb01g045720, SbSUT2 – Sb04g038030, SbSUT3 – Sb01g022430, SbSUT4 – Sb08g023310, SbSUT5 – Sb04g023860, SbSUT6 – Sb07g028120), *Triticum aestivum* (TaSUT1A, TaSUT1B, TaSUT1D), *Zea mays*** (ZmSUT1, ZmSUT2, ZmSUT3, ZmSUT4, ZmSUT5, ZmSUT6). Phylogenetic analysis was carried out using MUSCLE alignment, Gblocks curation followed by PhyML phylogeny (Dereeper et al., 2008) before viewing in Dendroscope (Huson et al., 2007). Accession numbers are shown along with gene identifications (*Brachypodium*, *Setaria*, and *Sorghum*). Asterisks indicate that the full genomic sequence is publicly available.
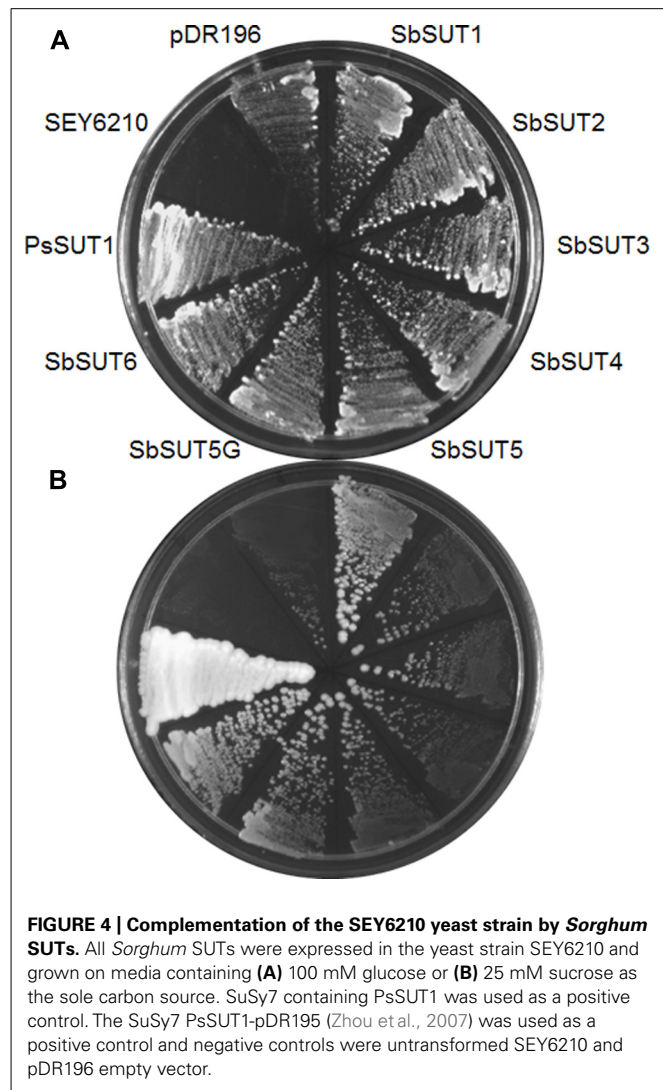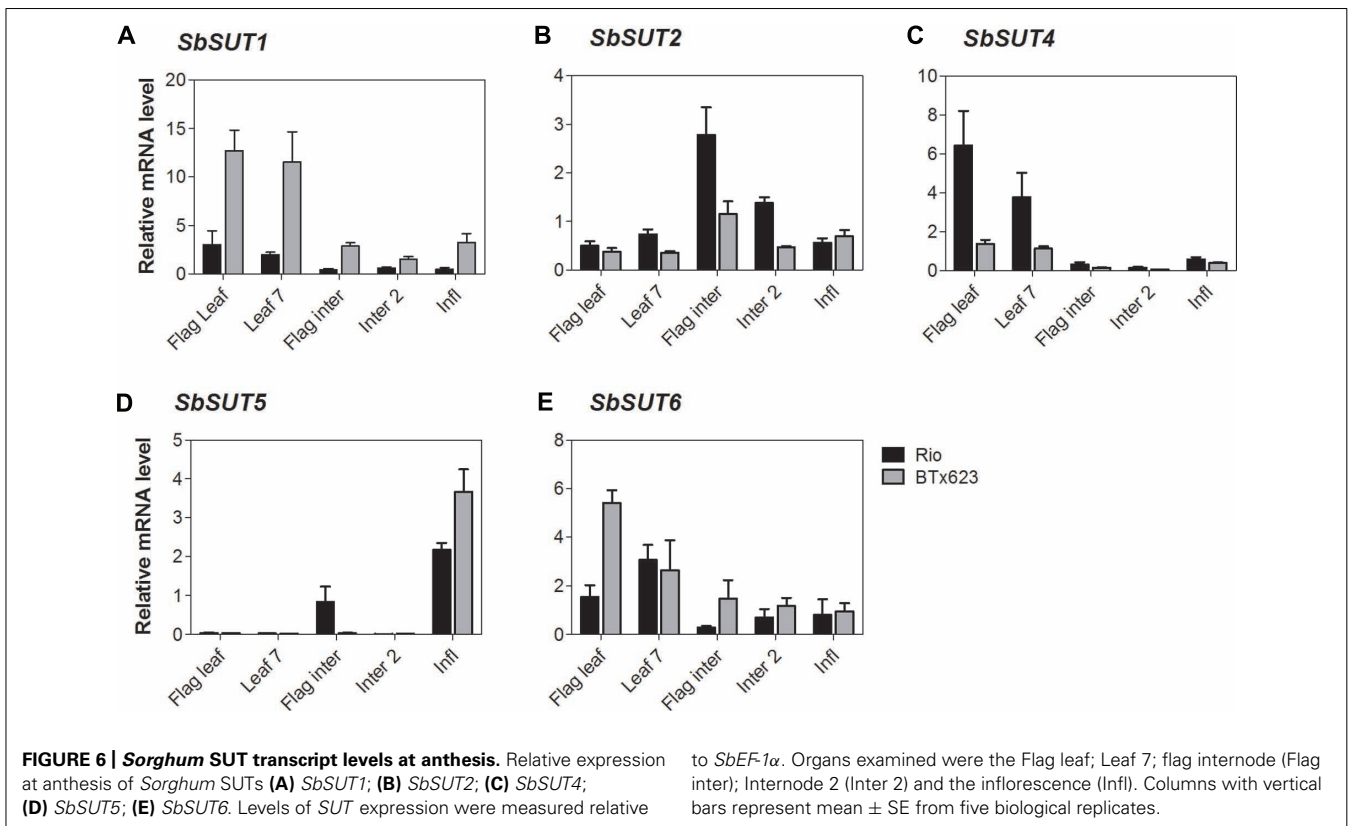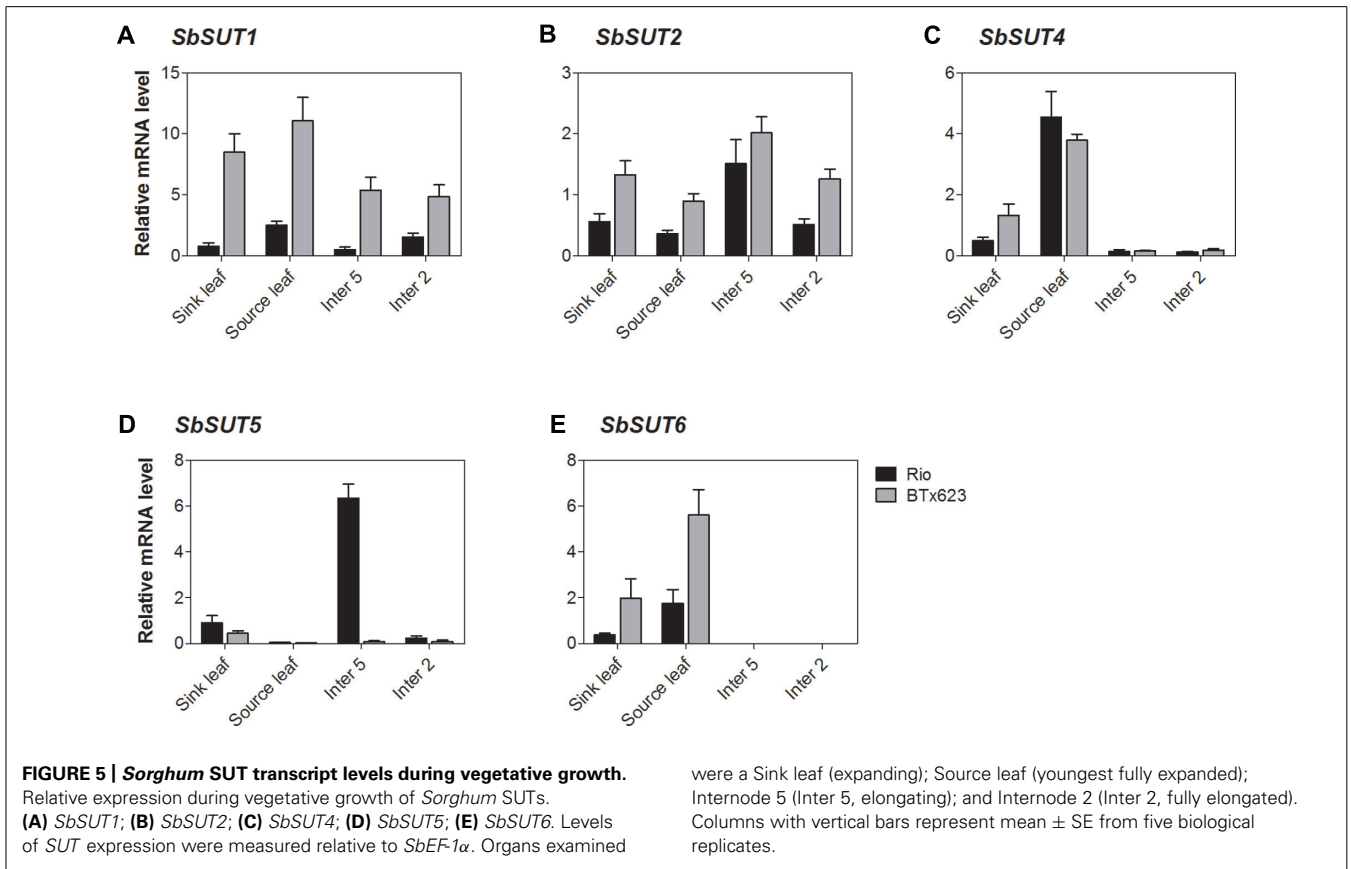

FIGURE 4 | Complementation of the SEY6210 yeast strain by *Sorghum* SUTs. All *Sorghum* SUTs were expressed in the yeast strain SEY6210 and grown on media containing **(A)** 100 mM glucose or **(B)** 25 mM sucrose as the sole carbon source. SuSy7 containing PsSUT1 was used as a positive control. The SuSy7 PsSUT1-pDR195 (Zhou et al., 2007) was used as a positive control and negative controls were untransformed SEY6210 and pDR196 empty vector.
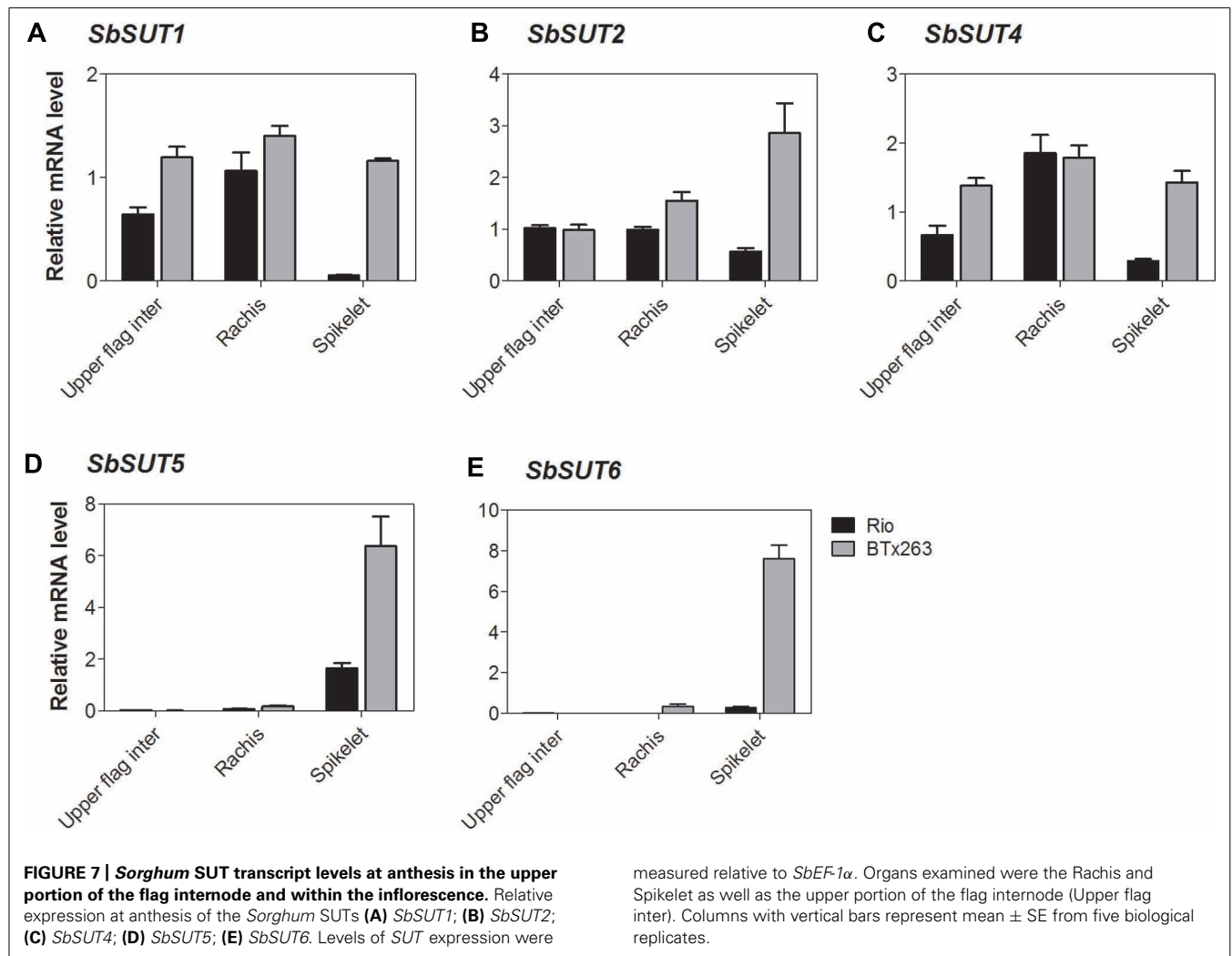
EXPRESSION OF *SUTs* IN YEAST

SUTs from cv. Rio were cloned and expressed in yeast using pDR195 or pDR196 yeast expression vectors (Rentsch et al., 1995), along with the *SbSUT5* from cv. BTx623. The SEY6210 strain of *Saccharomyces cerevisiae* supported growth on media containing sucrose as the sole carbon source, when complemented with each *SUT* (**Figure 4**). This indicates that the introduced SUT mediated sucrose import from the media to support yeast growth.

TRANSCRIPT LEVELS OF *SUTs*

All *SUTs* were expressed at measurable levels in all organs examined apart from *SbSUT3*, consistent with previous observations (Qazi et al., 2012). *SbSUT1* transcripts were detected in both source and sink organs with higher levels observed in cv. BTx623 compared to cv. Rio (two to threefold higher; **Figures 5A** and **6A**). During the vegetative stage of development, fully expanded leaves exhibited the highest level of expression, followed by expanding leaves and stems (**Figure 5A**). At anthesis, fully expanded leaves exhibited substantially higher (fourfold) levels of expression than
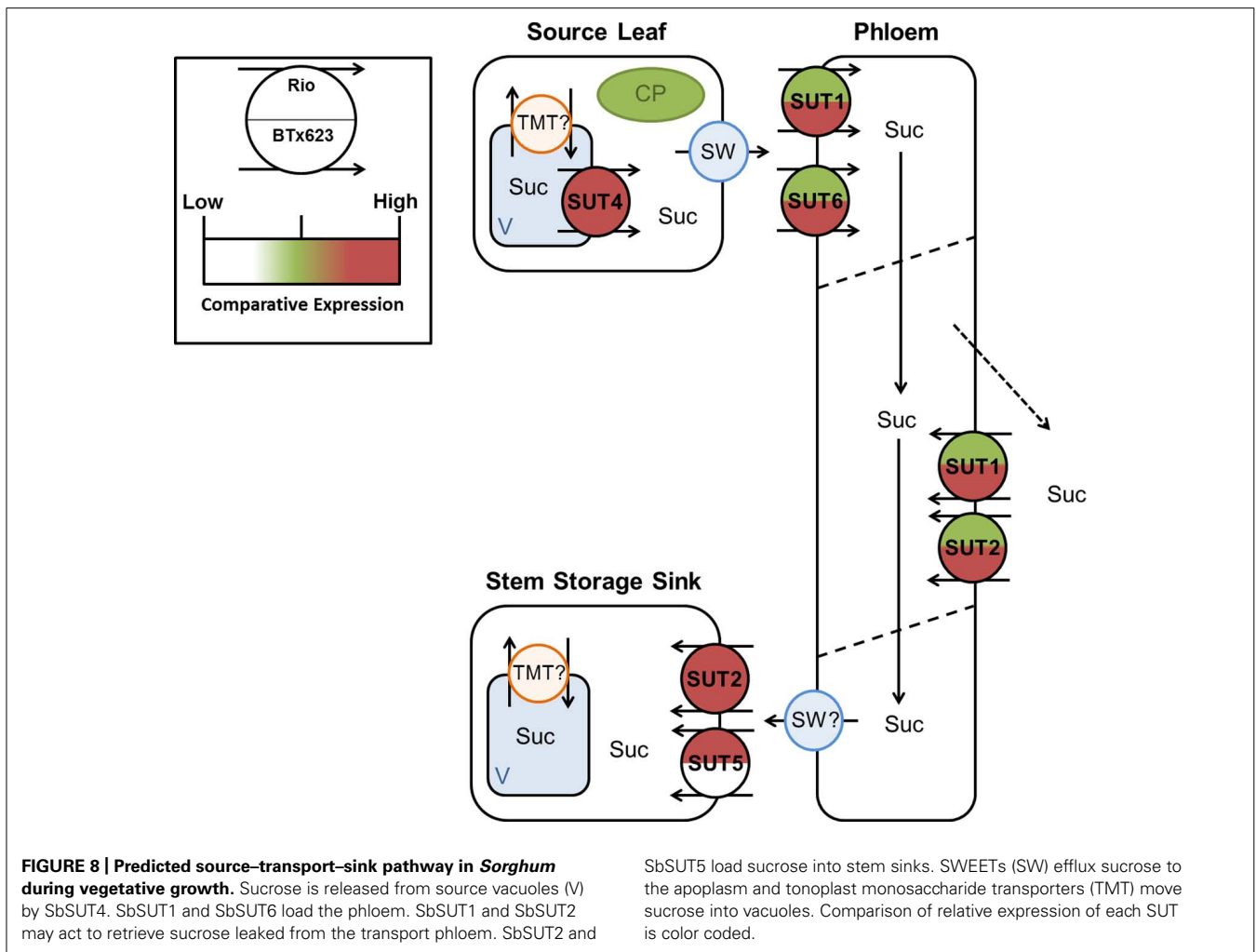
FIGURE 5 | *Sorghum* SUT transcript levels during vegetative growth.
Relative expression during vegetative growth of *Sorghum* SUTs.
(A) *SbSUT1*; **(B)** *SbSUT2*; **(C)** *SbSUT4*; **(D)** *SbSUT5*; **(E)** *SbSUT6*. Levels
of *SUT* expression were measured relative to *SbEF-1α*. Organs examined
were a Sink leaf (expanding); Source leaf (youngest fully expanded);
Internode 5 (Inter 5, elongating); and Internode 2 (Inter 2, fully elongated).
Columns with vertical bars represent mean ± SE from five biological
replicates.

FIGURE 6 | *Sorghum* SUT transcript levels at anthesis. Relative expression
at anthesis of *Sorghum* SUTs **(A)** *SbSUT1*; **(B)** *SbSUT2*; **(C)** *SbSUT4*;
(D) *SbSUT5*; **(E)** *SbSUT6*. Levels of *SUT* expression were measured relative
to *SbEF-1α*. Organs examined were the Flag leaf; Leaf 7; flag internode (Flag
inter); Internode 2 (Inter 2) and the inflorescence (Infl). Columns with vertical
bars represent mean ± SE from five biological replicates.

FIGURE 7 | *Sorghum* SUT transcript levels at anthesis in the upper portion of the flag internode and within the inflorescence. Relative expression at anthesis of the *Sorghum* SUTs **(A)** *SbSUT1*; **(B)** *SbSUT2*; **(C)** *SbSUT4*; **(D)** *SbSUT5*; **(E)** *SbSUT6*. Levels of *SUT* expression were measured relative to *SbEF-1α*. Organs examined were the Rachis and Spikelet as well as the upper portion of the flag internode (Upper flag inter). Columns with vertical bars represent mean ± SE from five biological replicates.

stems and inflorescences (**Figure 6A**). Expression levels were similar between cultivars in upper portions of their flag internodes along with rachis branches, but were greater in cv. BTx623 than cv. Rio in spikelets (**Figure 7A**). *SbSUT2* was expressed in all organs examined in both cultivars. During vegetative growth, expression was slightly higher in young elongating stems compared to other organs (**Figure 5B**). At anthesis, flag internodes had the highest levels of *SbSUT2* transcript with cv. Rio being twofold higher than cv. BTx623 (**Figure 6B**). Transcript levels were highest in the cv. BTx623 spikelets exhibiting a threefold difference compared to cv. Rio. Twofold higher levels of expression were observed in spikelets of cv. BTx623 than in rachis branches and upper portions of flag internodes of either cultivar (**Figure 7B**).

During vegetative growth, *SbSUT4* exhibited a similar pattern of expression in the two cultivars. *SbSUT4* expression was highest in fully expanded leaves, with at least twofold lower levels in other organs examined and especially so for stems (**Figure 5C**). In contrast, at anthesis, transcript levels of *SbSUT4* in source leaves were two to threefold greater in cv. Rio compared to cv. BTx623. Within inflorescences, *SbSUT4* transcripts were equally high in rachis branches but for spikelets, expression levels in cv. BTx623

exceeded those of cv. Rio by fourfold (**Figure 7C**). The cultivar difference was reflected, but to a lesser extent, in upper portions of their flag internodes (**Figure 7C**).

There was a clear trend in *SbSUT5* expression during the vegetative stage of development and at anthesis, and expression levels differed between cv. Rio and cv. BTx623 at both developmental stages. During vegetative growth, *SbSUT5* was strongly and exclusively expressed in elongating Internode 5 of cv. Rio (**Figure 5D**). At anthesis, the dominant level of expression switched to inflorescences with cv. BTx623 expression levels exceeding those of cv. Rio by ca 50% (**Figure 6D**). Within inflorescences, *SbSUT5* was expressed primarily in spikelets with threefold higher levels in cv. BTx623 compared to cv. Rio (**Figure 7D**). Transcripts were present in the flag internode of cv. Rio and absent in the same organ of cv. BTx623 (**Figure 6D**).

Transcripts of *SbSUT6* were only detected in sink and source leaves during vegetative growth with levels in cv. BTx623 being threefold greater than those of cv. Rio (**Figure 5E**). At anthesis, leaf expression dominance was retained with cultivar differences declining with leaf age (compare flag and leaf 7 – **Figure 6E**). However, low transcript levels were detected in stems

FIGURE 8 | Predicted source–transport–sink pathway in *Sorghum* during vegetative growth. Sucrose is released from source vacuoles (V) by SbSUT4. SbSUT1 and SbSUT6 load the phloem. SbSUT1 and SbSUT2 may act to retrieve sucrose leaked from the transport phloem. SbSUT2 and SbSUT5 load sucrose into stem sinks. SWEETs (SW) efflux sucrose to the apoplasm and tonoplast monosaccharide transporters (TMT) move sucrose into vacuoles. Comparison of relative expression of each SUT is color coded.

and inflorescences (**Figure 6E**). Within inflorescences, *SbSUT6* was strongly expressed in cv. BTx623 spikelets and either weakly expressed or absent from rachis branches and upper portions of flag internodes (**Figure 7E**).

DISCUSSION

The full genomic sequence of *Sorghum* has allowed identification of all *SbSUT* sequences in this model cereal monocot. Examination of *SbSUT* transcript levels in source leaves versus stem and inflorescence sinks provides a strong indication of the role each transporter may play in transporting sucrose from source leaves to these sinks. To further highlight these roles, two phenotypically different cultivars were used, BTx623 and Rio. BTx623 preferentially partitions sucrose to developing inflorescences and hence an emphasis on grain yield whilst cv. Rio stores sucrose in stem parenchyma cells similar to sugarcane. Collectively these analyzes begin to identify which SUTs may participate in phloem loading, axial phloem transport, and phloem unloading.

All six SbSUTs demonstrated complementation of the deficient yeast strain, SEY6210 (**Figure 4**), indicating they are sucrose transport competent, and likely to be functional *in planta*. The single amino acid sequence differences in SbSUT2 sequence between cultivars is predicted to lie in its N-terminal domain, as does the string of amino acids which vary in the SbSUT5 (see **Figure 2** and **Table 2**). The N-terminal domain has been shown to alter SUT affinity for sucrose (Schulze et al., 2000). In addition, recent evidence has identified particular amino acids in rice SUT1 which alters its transport activity (Reinders et al., 2012; Sun et al., 2012). However, these do not appear to correspond with amino acid differences we have identified between cv. BTx623 and cv. Rio (**Figure 2** and **Table 2**). Possible impacts of the detected SbSUT sequence differences between cultivars observed here need to be assessed experimentally.

In terms of phloem loading, based on their relative expression levels in source leaves, identified SbSUT4, SbSUT1, and SbSUT6 as potential candidates during vegetative and reproductive growth (see **Figures 5, 6, 8,** and **9**). For SbSUT4, this assertion is consistent with a high source leaf expression observed for *OsSUT2* (Eom et al., 2011) and *Populus tremula × alba* (gray poplar) *PtaSUT4* (Payyavula et al., 2011). A number of transporters belonging to the same phylogenetic group as SbSUT4 (see **Figure 3**), have been localized to the tonoplast. These include rice SUT2 (Eom et al., 2011), barley SUT2 (Endler et al., 2006; Group 4) and the dicotyledonous SUTs, AtSUT4 (Endler et al.,

FIGURE 9 | Predicted source–transport–sink pathway in *Sorghum* at anthesis. Sucrose is released from source vacuoles (V) by SbSUT4. SbSUT1 and SbSUT6 load the phloem. SbSUT1 and SbSUT2 may act to retrieve sucrose leaked from the transport phloem. SbSUT2 and SbSUT5 load sucrose into stem sinks. SbSUT5 and SbSUT6 load sucrose into reproductive sinks. SWEETs (SW) efflux sucrose to the apoplasm and tonoplast monosaccharide transporters (TMT) move sucrose into vacuoles. Comparison of relative expression of each SUT is color coded.

2006), *Lotus japonicus* LjSUT4 (Reinders et al., 2008), poplar PtaSUT4 (Payyavula et al., 2011), and tobacco NtSUT4 (Okubo-Kurihara et al., 2011). On the tonoplast, SUT4 functions to release sucrose from mesophyll vacuoles to their cytoplasm (Schulz et al., 2011; Schneider et al., 2012) rendering the vacuolar pool of sucrose available for phloem loading. The significance of this function for SUT4 is demonstrated by slowed photoassimilate export in knock down SUT4 mutants of rice (Eom et al., 2011).

SbSUT1 may play a role in apoplasmic phloem loading (**Figures 8** and **9**) as found for the closely related maize ZmSUT1 which also belongs to the C_4 NADP-ME subgroup (Slewinski et al., 2009). This assertion is based on finding that a maize *sut1* mutant exhibited a phenotype of shorter stature and carbohydrate accumulation in their source leaves (Slewinski et al., 2009). Consistent with this phenotype, the *sut1* mutant had a diminished ability to export sucrose from source leaves. Greater levels of *SbSUT1* transcript were detected in source leaves of cv. BTx623 than cv. Rio (**Figures 5A** and **6A**). These differences could reflect differences in sink demand between cultivars driving photosynthetic rate along with sucrose export from source leaves (Minchin et al., 2002; McCormick et al., 2006). *SbSUT6* is another phloem loading candidate (**Figures 8** and **9**). Similar to *SbSUT1*, transcript levels of *SbSUT6* were higher in source leaves of cv. BTx623 than cv. Rio at both vegetative and anthesis stages (**Figures 5E** and **6E**) supporting the notion that sink demand might be stronger in cv. BTx623.

In sweet *Sorghum*, sucrose is radially transferred from the phloem into stem storage parenchyma cells through a post-sieve element unloading pathway that likely includes an apoplasmic step (Tarpley and Vietor, 2007). In this context, *SbSUT2* and *SbSUT5* were highly expressed in internodes (**Figures 5B** and **6B**) where they may play a primary role in phloem unloading, retrieval of sucrose leaked from the phloem or phloem loading of sucrose remobilized from stem storage (**Figures 8** and **9**). However, since remobilization predominantly occurs during grain filling (Gutjahr et al., 2013), at anthesis SUTs likely function to facilitate radial transport of sucrose to stem storage pools or in retrieving sucrose leaked from the phloem.

Twofold greater expression of *SbSUT2* was observed in internodes of cv. Rio as opposed to those from cv. BTx623 at anthesis

(**Figure 6D**), suggesting this SUT may play an enhanced role in directing sucrose to stem storage parenchyma cells in cv. Rio. SbSUT2 has a predicted protein sequence of 594 amino acids, which is at least 60 amino acids longer than the five other *Sorghum* SUTs. Similarly, OsSUT4 has an extended central loop domain of around 90 amino acids and an extended N-terminal domain (Aoki et al., 2003). Little information is available for the other monocot Group 3 SUTs. However, an insertional mutant of the corresponding dicot SUT AtSUT3, showed no morphological phenotype (Barth et al., 2003).In comparison to the strong expression of *SbSUT5* in cv. Rio internodes (**Figures 5D** and **6D**), *SbSUT5* transcripts were absent from cv. BTx623 internodes. Rather *SbSUT5* transcripts were 1.5–2-fold higher in inflorescences of cv. BTx623 than cv. Rio (**Figure 6D**), and especially spikelets (**Figure 7D**). These expression patterns suggest that cv. BTx623 directs more sucrose toward development of reproductive structures than cv. Rio. *SbSUT6*, most closely related to *SbSUT5* (**Figure 3**), was strongly expressed within cv. BTx623 spikelets (**Figure 7E**) and hence may also contribute to inflorescence development (**Figure 9**).

Cultivar differences in expression profiles of *SbSUT5* were accompanied by the highest number of amino acid difference in SbSUT5 sequences (9 amino acids, **Table 2**). Little information is available about transporters belonging to Group 5 apart from *OsSUT5*. This gene exhibited broad expression across source and sink leaves as well as in developing grains of rice (Aoki et al., 2003). Similar to *SbSUT5*, SUT1 transporters of more distantly related C_3 species of rice, barley, and wheat appear to play a role in grain development. Antisense lines for *OsSUT1* showed little phenotypic difference when compared to wild-type in vegetative growth or differences in carbohydrate content of their source leaves (Ishimaru et al., 2001). However, grain filling was reduced substantially in *OsSUT1* antisense plants (Scofield et al., 2002). A number of other monocotyledonous plant SUT1 transporters also were found to be involved in grain development, including barley (Weschke et al., 2000) and wheat (Aoki et al., 2002) SUT1-type proteins. Whether *SbSUT1* plays a major role in grain development remains to be determined.

In conclusion, the six *Sorghum SUTs* were cloned from two cultivars that differ in carbohydrate partitioning. Expression analysis revealed that three of the *SUTs* were expressed strongly in source leaves (*SbSUT1*, *SbSUT4*, *SbSUT6*) and are likely to play roles in phloem loading. Two *SUTs* were expressed strongly in sinks (*SbSUT2*, *SbSUT5*) and are more likely to play roles in sink development and photoassimilate storage. *SbSUT3* was not detected in most organs examined. All of the *Sorghum* SUTs complemented the deficient yeast system, indicating they are sucrose transport competent. A number of amino acid sequence variations were identified between the SUTs from the two cultivars, and future functional characterization will determine if these variations result in alteration of their sucrose transport properties.

REFERENCES

Aoki, N., Hirose, T., Scofield, G. N., Whitfeld, P. R., and Furbank, R. T. (2003). The sucrose transporter gene family in rice. *Plant Cell Physiol.* 44, 223–232. doi: 10.1093/pcp/pcg030

Aoki, N., Whitfield, P., Hoeren, F., Scofield, G., Newell, K., Patrick, J., et al. (2002). Three sucrose transporter genes are expressed in the developing grain of hexaploid wheat. *Plant Mol. Biol.* 50, 453–462. doi: 10.1023/A:1019846832163

Barth, I., Meyer, S., and Sauer, N. (2003). PmSUC3: characterization of a SUT2/SUC3-type sucrose transporter from *Plantago major*. *Plant Cell* 15, 1375–1385. doi: 10.1105/tpc.010967

Berthier, A., Desclos, M., Amiard, V., Morvan-Bertrand, A., Demmig-Adams, B., Adams, W. W., et al. (2009). Activation of sucrose transport in defoliated *Lolium perenne* L.: an example of apoplastic phloem loading plasticity. *Plant Cell Physiol.* 50, 1329–1344. doi: 10.1093/pcp/pcp081

Blum, A., Sinmena, B., Mayer, J., Golan, G., and Shpiler, L. (1994). Stem reserve mobilization supports wheat-grain filling under heat-stress. *Aust. J. Plant Physiol.* 21, 771–781. doi: 10.1071/PP9940771

Blum, A., Golan, G., Mayer, J., and Sinmena, B. (1997). The effect of dwarfing genes on *sorghum* grain filling from remobilized stem reserves, under stress. *Field Crops Res.* 52, 43–54. doi: 10.1016/S0378-4290(96)03462-4

Braun, D. M., and Slewinski, T. L. (2009). Genetic control of carbon partitioning in grasses: roles of sucrose transporters and tie-dyed loci in phloem loading. *Plant Physiol.* 149, 71–81. doi: 10.1104/pp.108.129049

Dereeper, A., Guignon, V., Blanc, G., Audic, S., Buffet, S., Chevenet, F., et al. (2008). Phylogeny.fr: robust phylogenetic analysis for the non-specialist. *Nucleic Acids Res.* 36, W465–W469. doi: 10.1093/nar/gkn180

Dohmen, R. J., Strasser, A. W. M., Honer, C. B., and Hollenberg, C. P. (1991). An efficient transformation procedure enabling long-term storage of competent cells of various yeast genera. *Yeast* 7, 691–692. doi: 10.1002/yea.320070704

Endler, A., Meyer, S., Schelbert, S., Schneider, T., Weschke, W., Peters, S. W., et al. (2006). Identification of a vacuolar sucrose transporter in barley and *Arabidopsis* mesophyll cells by a tonoplast proteomic approach. *Plant Physiol.* 141, 196–207. doi: 10.1104/pp.106.079533

Eom, J. S., Cho, J. I., Reinders, A., Lee, S. W., Yoo, Y., Tuan, P. Q., et al. (2011). Impaired function of the tonoplast-localized sucrose transporter in rice, OsSUT2, limits the transport of vacuolar reserve sucrose and affects plant growth. *Plant Physiol.* 157, 109–119. doi: 10.1104/pp.111.176982

Gutjahr, S., Vaksmann, M., Dingkuhn, M., Thera, K., Trouche, G., Braconnier, S., et al. (2013). Grain, sugar and biomass accumulation in tropical sorghums. I. Trade-offs and effects of phenological plasticity. *Funct. Plant Biol.* 40, 342–354. doi: 10.1071/FP12269

Hoffmann-Thoma, G., Hinkel, K., Nicolay, P., and Willenbrink, J. (1996). Sucrose accumulation in sweet *sorghum* stem internodes in relation to growth. *Physiol. Plant.* 97, 277–284. doi: 10.1034/j.1399-3054.1996.970210.x

Huson, D. H., Richter, D. C., Rausch, C., Dezulian, T., Franz, M., and Rupp, R. (2007). Dendroscope: an interactive viewer for large phylogenetic trees. *BMC Bioinformatics* 8:460. doi: 10.1186/1471-2105-8-460

Ishimaru, K., Hirose, T., Aoki, N., Takahashi, S., Ono, K., Yamamoto, S., et al. (2001). Antisense expression of a rice sucrose transporter OsSUT1 in rice (*Oryza sativa* L.). *Plant Cell Physiol.* 42, 1181–1185. doi: 10.1093/pcp/pce148

Jacobsen, K. R., Fisher, D. G., Maretzki, A., and Moore, P. H. (1992). Developmental changes in the anatomy of the sugarcane stem in relation to phloem unloading and sucrose storage. *Bot. Acta* 105, 70–80.

Lalonde, S., Wipf, D., and Frommer, W. B. (2004). Transport mechanisms for organic forms of carbon and nitrogen between source and sink. *Annu. Rev. Plant Biol.* 55, 341–372. doi: 10.1146/annurev.arplant.55.031903.141758

Lemoine, R. (2000). Sucrose transporters in plants: update on function and structure. *Biochim. Biophys. Acta* 1465, 246–262. doi: 10.1016/S0005-2736(00)00142-5

Lingle, S. E. (1987). Sucrose metabolism in the primary culm of sweet sorghum during development. *Crop Sci.* 27, 1214–1219. doi: 10.2135/cropsci1987.0011183X002700060025x

Lu, J. M. Y., and Bush, D. R. (1998). His-65 in the proton-sucrose symporter is an essential amino

acid whose modification with site-directed mutagenesis increases transport activity. *Proc. Natl. Acad. Sci. U.S.A.* 95, 9025–9030. doi: 10.1073/pnas.95.15.9025

McCormick, A. J., Cramer, M. D., and Watt, D. A. (2006). Sink strength regulates photosynthesis in sugarcane. *New Phytol.* 171, 759–770. doi: 10.1111/j.1469-8137.2006.01785.x

Minchin, P. E. H., Thorpe, M. R., Farrar, J. F., and Koroleva, O. A. (2002). Source–sink coupling in young barley plants and control of phloem loading. *J. Exp. Bot.* 53, 1671–1676. doi: 10.1093/jxb/erf003

Murray, S. C., Rooney, W. L., Mitchell, S. E., Sharma, A., Klein, P. E., Mullet, J. E., et al. (2008). Genetic improvement of *Sorghum* as a biofuel feedstock: II. QTL for stem and leaf structural carbohydrates. *Crop Sci.* 48, 2180–2193. doi: 10.2135/cropsci2008.01.0068

Okubo-Kurihara, E., Higaki, T., Kurihara, Y., Kutsuna, N., Yamaguchi, J., and Hasezawa, S. (2011). Sucrose transporter NtSUT4 from tobacco BY-2 involved in plant cell shape during miniprotoplast culture. *J. Plant Res.* 124, 395–403. doi: 10.1007/s10265-010-0377-7

Payyavula, R. S., Tay, K. H. C., Tsai, C. J., and Harding, S. A. (2011). The sucrose transporter family in *Populus*: the importance of a tonoplast PtaSUT4 to biomass and carbon partitioning. *Plant J.* 65, 757–770. doi: 10.1111/j.1365-313X.2010.04463.x

Pazdernik, N. J., Matzke, E. A., Jessen-Marshall, A. E., and Brooker, R. J. (2000). Roles of charged residues in the conserved motif, G-X-X-X-D/E-R/K-X-G-[X]-R/K-R/K, of the lactose permease of *Escherichia coli*. *J. Membr. Biol.* 174, 31–40. doi: 10.1007/s002320001029

Preisser, J., and Komor, E. (1991). Sucrose uptake into vacuoles of sugarcane suspension cells. *Planta* 186, 109–114. doi: 10.1007/BF00201505

Qazi, H. A., Paranjpe, S., and Bhargava, S. (2012). Stem sugar accumulation in sweet *sorghum* – activity and expression of sucrose metabolizing enzymes and sucrose transporters. *J. Plant Physiol.* 169, 605–613. doi: 10.1016/j.jplph.2012.01.005

Reinders, A., Sivitz, A. B., Starker, C. G., Gantt, J. S., and Ward, J. M. (2008). Functional analysis of LjSUT4, a vacuolar sucrose transporter from *Lotus japonicus*. *Plant Mol. Biol.* 68, 289–299. doi: 10.1007/s11103-008-9370-0

Reinders, A., Sun, Y., Karvonen, K. L., and Ward, J. M. (2012). Identification of amino acids important for substrate specificity in sucrose transporters using gene shuffling. *J. Biol. Chem.* 287, 30296–30304. doi: 10.1074/jbc.M112.372888

Rentsch, D., Laloi, M., Rouhara, I., Schmelzer, E., Delrot, S., and Frommer, W. B. (1995). NTR1 encodes a high-affinity oligopeptide transporter in *Arabidopsis*. *FEBS Lett.* 370, 264–268. doi: 10.1016/0014-5793(95)00853-2

Robinson, J. S., Klionsky, D. J., Banta, L. M., and Emr, S. D. (1988). Protein sorting in *Saccharomyces cerevisiae*: isolation of mutants defective in the delivery and processing of multiple vacuolar hydrolases. *Mol. Cell. Biol.* 8, 4936–4948.

Saftner, R. A., Daie, J., and Wyse, R. E. (1983). Sucrose uptake and compartmentation in sugar-beet taproot tissue. *Plant Physiol.* 72, 1–6. doi: 10.1104/pp.72.1.1

Schneider, S., Hulpke, S., Schulz, A., Yaron, I., Holl, J., Imlau, A., et al. (2012). Vacuoles release sucrose via tonoplast-localised SUC4-type transporters. *Plant Biol.* 14, 325–336. doi: 10.1111/j.1438-8677.2011.00506.x

Schulz, A., Beyhl, D., Marten, I., Wormit, A., Neuhaus, E., Poschet, G., et al. (2011). Proton-driven sucrose symport and antiport are provided by the vacuolar transporters SUC4 and TMT1/2. *Plant J.* 68, 129–136. doi: 10.1111/j.1365-313X.2011.04672.x

Schulze, W., Weise, A., Frommer, W. B., and Ward, J. M. (2000). Function of the cytosolic N-terminus of sucrose transporter AtSUT2 in substrate affinity. *FEBS Lett.* 485, 189–194. doi: 10.1016/S0014-5793(00)02180-3

Scofield, G. N., Hirose, T., Gaudron, J. A., Upadhyaya, N. M., Ohsugi, R., and Furbank, R. T. (2002). Antisense suppression of the rice sucrose transporter gene, OsSUT1, leads to impaired grain filling and germination but does not affect photosynthesis. *Funct. Plant Biol.* 29, 815–826. doi: 10.1071/PP01204

Slewinski, T. L., Meeley, R., and Braun, D. M. (2009). Sucrose transporter1 functions in phloem loading in maize leaves. *J. Exp. Bot.* 60, 881–892. doi: 10.1093/jxb/ern335

Spyropoulos, I. C., Liakopoulos, T. D., Bagos, P. G., and Hamodrakas, S. J. (2004). TMRPres2D: high quality visual representation of trans-membrane protein models. *Bioinformatics* 20, 3258–3260. doi: 10.1093/bioinformatics/bth358

Sun, Y., Lin, Z., Reinders, A., and Ward, J. M. (2012). Functionally important amino acids in rice sucrose transporter OsSUT1. *Biochemistry* 51, 3284–3291. doi: 10.1021/bi201934h

Tarpley, L., and Vietor, D. M. (2007). Compartmentation of sucrose during radial transfer in mature *sorghum* culm. *BMC Plant Biol.* 7:33. doi: 10.1186/1471-2229-7-33

Weschke, W., Panitz, R., Sauer, N., Wang, Q., Neubohn, B., Weber, H., et al. (2000). Sucrose transport into barley seeds: molecular characterization of two transporters and implications for seed development and starch accumulation. *Plant J.* 21, 455–467. doi: 10.1046/j.1365-313x.2000.00695.x

Williams, L., Thom, M., and Maretzki, A. (1990). Characterization of a proton translocating ATPase and sucrose uptake in a tonoplast-enriched vesicle fraction from sugarcane. *Physiol. Plant.* 80, 169–176. doi: 10.1111/j.1399-3054.1990.tb04392.x

Yamada, K., Osakabe, Y., Mizoi, J., Nakashima, K., Fujita, Y., Shinozaki, K., et al. (2010). Functional analysis of an *Arabidopsis thaliana* abiotic stress-inducible facilitated diffusion transporter for monosaccharides. *J. Biol. Chem.* 285, 1138–1146. doi: 10.1074/jbc.M109.054288

Zhao, Y. L., Dolat, A., Steinberger, Y., Wang, X., Osman, A., and Xie, G. H. (2009). Biomass yield and changes in chemical composition of sweet *sorghum* cultivars grown for biofuel. *Field Crops Res.* 111, 55–64. doi: 10.1016/j.fcr.2008.10.006

Zhou, Y. C., Qu, H. X., Dibley, K. E., Offler, C. E., and Patrick, J. W. (2007). A suite of sucrose transporters expressed in coats of developing legume seeds includes novel pH-independent facilitators. *Plant J.* 49, 750–764. doi: 10.1111/j.1365-313X.2006.03000.x